Available online at www.sciencedirect.com

ScienceDirect

Procedia Structural Integrity 11 (2018) 314–321

Structural Integrity Procedia

www.elsevier.com/locate/procedia

XIV International Conference on Building Pathology and Constructions Repair – CINPAR 2018

Iconic crumbling of the clock tower in Amatrice after 2016 central Italy seismic sequence: advanced numerical insight

M. Poiani[a]*, V. Gazzani[a], F. Clementi[a], G. Milani[b], M. Valente[b], S. Lenci[a]

[a]*Department of Civil and Building Engineering, and Architecture, Polytechnic University of Marche, Via Brecce Bianche, 60131, Ancona, Italy*
[b]*Department of Architecture, Built Environment and Construction Engineering ABC, Politecnico di Milano, Piazza Leonardo da Vinci 32, 20133, Milan, Italy,*

Abstract

The present paper investigates from an advanced numerical point of view the progressive damage of the Amatrice (Rieti, Italy) civic clock tower, after a long sequence of strong earthquakes that struck central Italy in 2016. Two advanced numerical models are here utilised to have an insight into the modalities of progressive damage and the behaviour of the structure under strong non-linear dynamic excitations, namely a Non-Smooth Contact Dynamics (NSCD) and a FE Concrete Damage Plasticity (CDP) models. In both cases, a full 3D detailed discretization is adopted. From the numerical results, both the role played by the actual geometries and the insufficient resistance of the constituent materials are envisaged, showing a good match with actual crack patterns observed after the seismic sequence.

Peer-review under responsibility of the CINPAR 2018 organizers

Keywords: Non-linear dynamic analyses; Non-Smooth Contact Dynamics method; Concrete Damage Plasticity model; Masonry tower.

1. Introduction

The seismic events, which hit Central Italy on 24th August 2016, 26th and 30th October 2016 and 18th January 2017, have caused casualties and significant damage mostly to buildings and architectural heritage of the Italian regions of Marche, Lazio, Abruzzo and Umbria. The mainshock occurred on 24th August at 3:36 am (local time) with epicentre close to Accumoli (Rieti province) and with a magnitude M_w= 6.2; it was followed, at 4.33 am, by an aftershock with

* Corresponding author.
E-mail address: m.poiani@pm.univpm.it

Peer-review under responsibility of the CINPAR 2018 organizers
10.1016/j.prostr.2018.11.041

epicentre close to Norcia (Perugia province) and with a magnitude M_w= 5.5. These events caused a total of 299 fatalities, 386 injured and about 4800 homeless (Fiorentino et al., 2018; Italian Department of Civil Protection, 2017).

On 26th October, there were two strong aftershocks with 5.6 and 6.1 M_w. The earthquake of 30th October, which happened at 07:40 am with M_w 6.5, is the largest event in terms of released energy occurred in Italy since the M_w 6.9 in 1980 during the Irpinia earthquake and, after this quake, many small towns were heavily damaged (Clementi et al., 2016b; F. Clementi et al., 2017b, 2017c). Finally, on 18th January 2017 took place a new sequence of four strong shocks of M_w=5 and epicentres located between the cities of Montereale, Capitignano and Cagnano Amiterno.

Icon of damage and destruction of a long sequence of strong earthquakes of 2016-2017 is the Amatrice civic clock tower which will be investigated in this paper. Two advanced numerical models are here utilised to have an insight into the modalities of progressive damage and to provide a picture of the actual behaviour of the structure.

2. The Amatrice clock tower: historical and geometrical surveys

Symbol of the city of Amatrice (Rieti, Italy), the Civic Tower (Fig. 1) rises in Cacciatori del Tevere square, underlining the crossroads of two main streets of the city centre, Via Roma and Corso Umberto I. There are few historical data about the Civic Tower, its origins are placed back to medieval times, as early as 1293 it was mentioned in ancient documents. Originally the clock tower was connected to the Church of Santa Lucia, demolished in 1684 by the feudal "lord" Alessandro Maria Orsini: on this occasion, the base of the tower was reinforced and a small annex was added on two sides. The last and probably the only consolidation intervention was carried out on the tower in 1979, when, following the earthquake of the Alta Valnerina (central Italy), significant damage was noticed to the tower. In 1985 the original bell of 1494 was replaced because it had undergone a crack during the restoration phases: a lighter one has been inserted in the tower to avoid high oscillations as in the past.

From a geometrical point of view, the civic tower of Amatrice has a rectangular plan of 4.00 m x 5.30 m and a height of about 25 m. At the base, there is a small overhang leaning only two walls, to east elevation with a depth of 1.5 m, and to north elevation with a depth of 0.60 m. The annex houses the staircase leading to the entrance of upper floors. In its vertical development there are three distinct areas marked by the reduction of the wall thickness. The first floor is located at about 9 m in height and it is composed of smoothed stones on the outer side, falling 15 centimeters in the wall thickness, while the second frame is located at the height of about 19 meters and it marks the passageway from the tower to the belfry. In its highest part, there is the bell cell which develops longitudinally for just over 5 m: it consists of 4 regular piers with dimension 0.90 m x 0.80 m and with same openings on the opposite sides (see Fig. 1). In the top, Amatrice clock tower has a wooden pavilion roof.

Fig. 1. Main façades of Civic Tower of Amatrice and historical photos of Corso Umberto I.

3. The model

In this section, the principal peculiarities of Non-Smooth Contact Dynamics (NSCD) and FE Concrete Damage Plasticity (CDP) models and the main modelling assumptions are highlighted. The problem parameters and seismic excitation applied to the base of the civic tower are also briefly reported.

3.1. Non-Smooth Contact Dynamics method

The dynamics of a system of rigid bodies is governed by the equation of motion and by the frictional contact conditions. To describe the frictional contact laws, we have to introduce some basic definitions. In the following, the notation adopted in (Jean, 1999) is used (scalars, vectors, and tensors are explicitly declared, and italic letters are used for all of them). Given two arbitrary bodies B_i and B_j, let P_i and P_j (Fig. 2a) be the points of possible contact on the boundaries of B_i and B_j, respectively, and let n be the outer unit vector, orthogonal to the boundary of B_i in P_i. We define $g = (P_j - P_i)\cdot n$ the gap between P_i and P_j (a dot means scalar product), $(\dot{u}_n; \dot{u}_t)$ the normal and tangential velocities of P_j with respect to P_i, and (r_n, r_t) the normal and tangential reactive forces of B_i on B_j.

The contact conditions are:

1. The Signorini's law of impenetrability (Fig. 2b)

$$g \geq 0, r_n \geq 0, g r_n = 0, \tag{1}$$

which, in the case of contact $g = 0$, is equivalent to the following Kuhn–Tucker conditions (Moreau, 1988)

$$\dot{u}_n \geq 0, r_n \geq 0, \dot{u}_n r_n = 0, \tag{2}$$

written in term of relative normal velocity.

2. The dry-friction Coulomb's law (Fig. 2c) that governs the behaviour in the tangential direction

$$|r_n| \leq \mu r_n; \begin{cases} r_t < \mu r_n \rightarrow \dot{u}_t = 0 \\ |r_t| = \mu r_n \rightarrow \dot{u}_t = -\lambda \frac{r_t}{|r_t|} \end{cases}, \tag{3}$$

with μ the friction coefficient and λ an arbitrary positive real number.

If q is the vector of the system configuration parameters (unknown translations and rotations of each body) and p is the global vector of reaction forces, the equation of motion can be written as follows

$$M\ddot{q} = f(q, \dot{q}, t) + p, \tag{4}$$

where M is the mass matrix, and f is the vector of external forces.

The local pairs $(\dot{u}_n; \dot{u}_t)$ and (r_n, r_t), characteristic of each contact, are related to the global vectors $\dot{q}$ and p, respectively, through linear maps which depend on q. Since the contact laws (1) - (3) are non-smooth, velocities $\dot{q}$ and reactions p are discontinuous functions of time. They belong to the set of bounded variation functions, i.e. functions which, at each time, have finite left and right limits. Since the accelerations are not defined when the velocities are discontinuous, Eq. (4) is reformulated in integral form (Jean, 1999; Moreau, 1988), and it is solved numerically using a time-stepping approach, where t time is discretized into time intervals, and, within each time interval $[t_i, t_{i+1}]$, the equation of motion is integrated as follows

$$M(\dot{q}_{i+1} - \dot{q}_i) = \int_{t_i}^{t_{i+1}} f(q, \dot{q}, t) dt + \bar{p}_{i+1}, \tag{5a}$$

$$q_{i+1} = q_i + \int_{t_i}^{t_{i+1}} \dot{q}(t) dt. \tag{5b}$$

Where $\bar{p}_{i+1}$ is the impulse in $[t_i; t_{i+1}]$. The primary variables of the problem are the velocity vector $\dot{q}_{i+1}$ and the impulse vector $\bar{p}_{i+1}$ at the instant t_{i+1}. In NSCD method, the integrals in (5a) and (5b) are evaluated by means of an implicit time integrator. The overall set of global Eq. (5a) and (5b) and local contact relations (1) and (2), where the reactions are approximated by the average impulses in $[t_i; t_{i+1}]$, is condensed at the contact local level, and then they are solved by means of a non-linear Gauss–Seidel by block method.

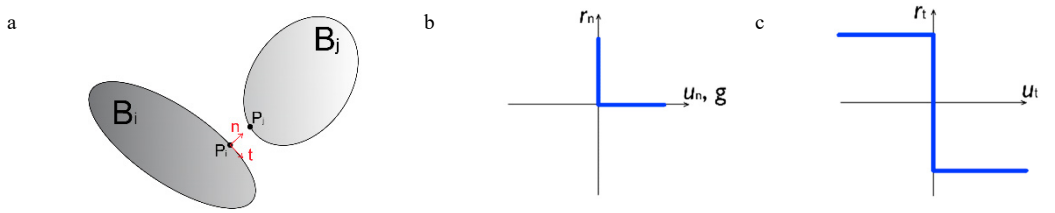

Fig. 2. (a) The interaction between two bodies; (b) Signorini's law; (c) Coulomb's law.

The relations (1) imply perfectly plastic impact, i.e., the Newton law with restitution coefficient equal to zero. A perfect plastic impact law makes impossible to describe bouncing phenomena, and, furthermore, overestimates the energy dissipated during impacts. However, in case of systems of bricks or stones, the restitution coefficient has low values, and bouncing phenomena can be neglected. Since we are interested in the dynamical interactions between different parts of the civic clock tower, we neglect blocks deformability. It follows that the numerical results obtained depict an overall picture of the tower dynamics and they portray the failure mechanisms of the whole tower, due to blocks rocking and sliding, but they do not describe the stresses and strain distributions within each block.

The values of friction coefficient μ range from 0.3 to 1.2, according to different combinations of units and mortars (Vasconcelos and Lourenço, 2009). As a first attempt, we assume the value μ = 0.5 for the interface block/block, and μ = 0.9 for the interface block/foundation to observe, mainly, the dynamics of the tower without the structure-foundation interaction.

Furthermore, it is important to underline that in real old masonry buildings, the degradation of the mortar over time contributes to deteriorate the friction coefficient and this confirms the hypothesis of first attempt. Finally, we note that damping is not considered here and only friction and perfect plastic impacts dissipate energy.

3.2. Concrete Damage Plasticity method

Three-dimensional finite element models of the tower are also created and non-linear dynamic analyses are conducted using computer code Abaqus©, assuming for masonry a CDP material model (Lee and Fenves, 1998). Although a CDP approach is conceived for isotropic brittle materials like concrete, it has been widely shown that its basic constitutive law can be also adapted to masonry, see e.g. (Acito et al., 2014; Valente and Milani, 2016).

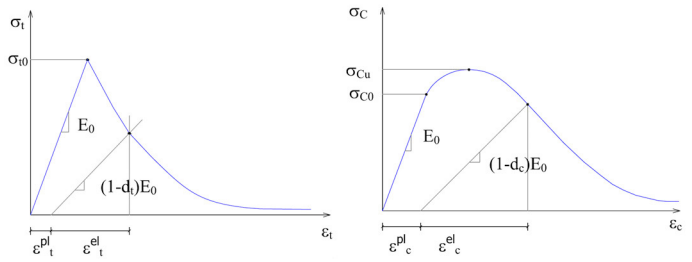

Fig. 3. Constitutive laws in tension and compression adopted for masonry.

CDP model allows to analyse materials with different strengths in tension and compression, assuming distinct damage parameters. In tension, see Fig. 3, the stress-strain response follows a linear elastic relationship until the peak stress σ_{t0} is reached. Then, micro-cracks start to propagate in the material, a phenomenon that is macroscopically represented by softening in stress-strain relationship. Under axial compression, the response is linear up to the value of the yield

stress σ_{c0}. After the yield stress, the response is typically characterised by hardening, which anticipates compression crushing, represented by a softening branch beyond the peak stress σ_{cu} (parabolic softening law).

The damage variables in tension d_t and in compression d_c are defined using the following relationships:

$$\sigma_t = (1 - d_t)E_0\left(\varepsilon_t - \varepsilon_t^{pl}\right),$$

$$\sigma_c = (1 - d_c)E_0\left(\varepsilon_c - \varepsilon_c^{pl}\right), \tag{6}$$

where $\sigma_t(\sigma_c)$ is the mono-axial tensile (compressive) stress, E_0 is the initial elastic modulus, $\varepsilon_t(\varepsilon_c)$ is the total strain in tension (compression), $\varepsilon_t^{pl}\left(\varepsilon_c^{pl}\right)$ is the equivalent plastic strain in tension (compression). In this study, damage is assumed active in tension only, since the tensile strength of the material is very low in comparison with the compressive one. When strain reaches a critical value, the material elastic modulus degrades in the unloading phase to $E<E_0$. In the numerical simulations a reduction equal to 5% of Young modulus with respect to the initial value is assumed for a plastic deformation equal to 0.003.

The strength domain is a standard Drucker–Prager surface modified with a so-called K_c parameter kept equal to 0.667, see Fig. 4a, representing the ratio between the distance from the hydrostatic axis of the maximum compression and tension, respectively. The tension corner is regularised with a correction parameter referring to eccentricity, see Fig. 4b. User's guide suggests a default value of 0.1. A value of 10° is adopted for the dilatation angle for the inelastic deformation in non-linear range, which is in agreement with the data suggested in (Pluijm et al., 2000). The ratio between the bi-axial (f_{bo}) and mono-axial (f_{co}) compression strength has been kept equal to 1.16 as suggested in the literature, (Dhanasekar et al., 1985) (Milani et al., 2006), for concrete (masonry behaviour found to be similar).

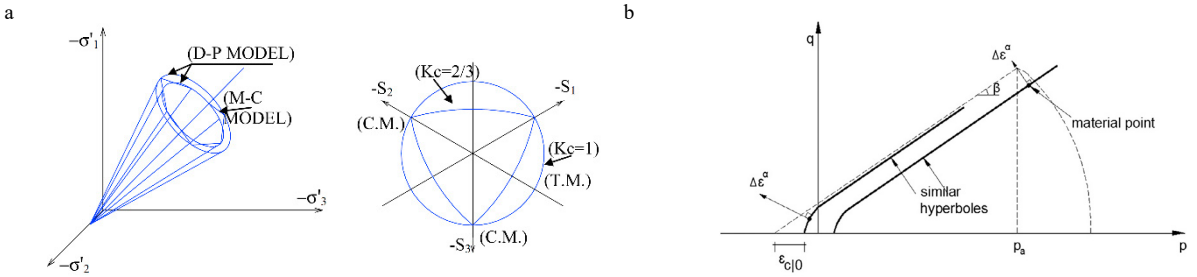

Fig. 4. (a) 3D strength domain adopted in Abaqus© for CDP model and meaning of Kc parameter. D–P: Drucker Prager strength criterion. M–C: Mohr-Coulomb strength criterion. C.M.: compressive meridian. T.M.: tensile meridian; (b) Smoothed Druker-Prager failure criterion *p*–*q* plane.

The values adopted for cohesion and masonry elastic modulus are taken in agreement with Explicative Notes (Circolare Ministeriale n. 617, 2009) of the Italian code, assuming two different masonry typology constituted by disordered rubble stone masonry to take into account the different size of the ashlars. The first material, used for main parts of tower, has E=1600 MPa, f_m=6 MPa and f_{tm}=0.09 MPa, while the second material, utilised for the annex and for the bell cell, has E=1400 MPa, f_m=4.5 MPa and f_{tm}=0.08 MPa.

3.3. Discretization schemes and analysis settings

The geometrical complexity of Amatrice civic clock tower requires some geometrical simplifications, being impossible to reproduce the real layout of the masonry walls, made by brick fragments and ashlars of small size as shown in Fig. 1. First of all, thanks to repeated dynamic tests of various earthquakes (as reported in the Introduction) it is possible to establish that the masonry can be considered as a one-leaf-masonry until failure. This fact permits us to utilise a continuous approach using Abaqus© and FE CDP model as shown in Fig. 5a. The FE model is composed of 95612 elements and 20898 nodes and it is fixed at the base.

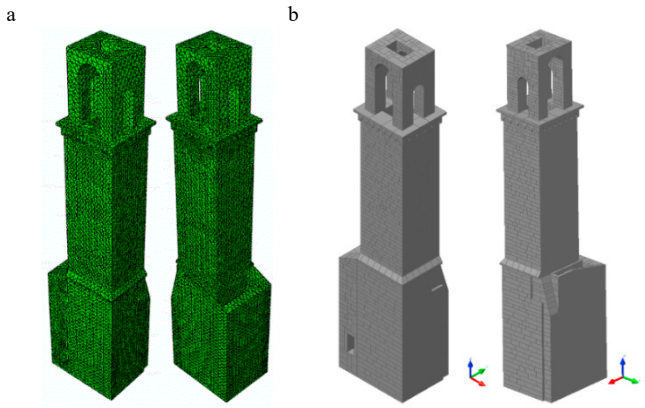

Fig. 5. (a) FE discretization of the tower in Abaqus©, (b) blocks distribution for the geometrical scheme of clock tower in LMGC90©.

Otherwise, with the final aim of confirming what occurred following the seismic shocks, it was decided to use an accurate mapping of the masonry as it is possible to see from Fig. 1 with the discontinuous approach using the code LMGC90©. The size of the blocks (Fig. 5b) used is directly taken up by the reliefs of the facades, while the internal wall texture has been hypothesised. Only in the presence of very small and irregular ashlars, typically at the top of the belfry and in the annex walls, we have used larger dimensions than relief, merely merging up to five (small) adjacent blocks. The rounded geometry of the blocks has been regularised using straight vertical and horizontal surfaces to avoid further computational burdens. Finally, the numerical model is composed of 2899 rigid blocks with different geometries.

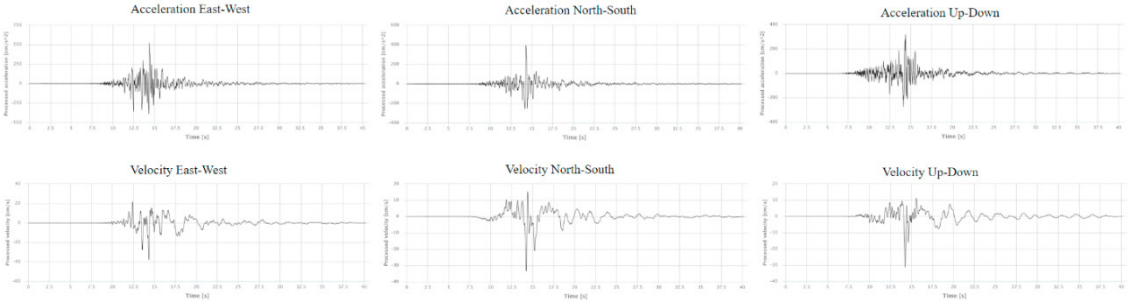

Fig. 6. Seismic accelerations and velocities applied to the foundation in the three coordinate directions.

Concerning the seismic loading, the accelerations and velocities of Amatrice (Rieti, Italy) of the 30th October 2016 earthquake have been considered. During that earthquake in Amatrice (AMT recording Station) a Peak Ground Acceleration (PGA) of 521.618 cm/s^2 and a Peak Ground Velocity (PGV) of 37.915 cm/s have been registered (see the website: http:// http://itaca.mi.ingv.it). In numerical simulations, accelerations are applied to FE model and velocities are applied to DE model at the base where the tower is laid. The three velocities components in the three main coordinate directions are determined by direct integration of the accelerations in a time interval of 40 s, during which the maximum amplitudes are attained, without the use of any correlation method. Both accelerations and velocities are represented in Fig. 6. During simulations, time step dt = 0.005 s has been used.

3.4. Preliminary results of numerical analyses

The first numerical results with NSCD method are reported in Fig. 7 for different time steps. With the above data, the tower collapses at the bell cell, where the overturning mechanism is favoured by the presence of non-regular and small-sized materials. The bell blocks motion occurs in the first 15 s of the seismic excitation, during which the largest velocity peaks are attained. For time instants larger than 20 s, the tower stays at rest, since the velocity peaks of the seismic excitation are not sufficiently large to activate other blocks sliding and/or rotation mechanisms.

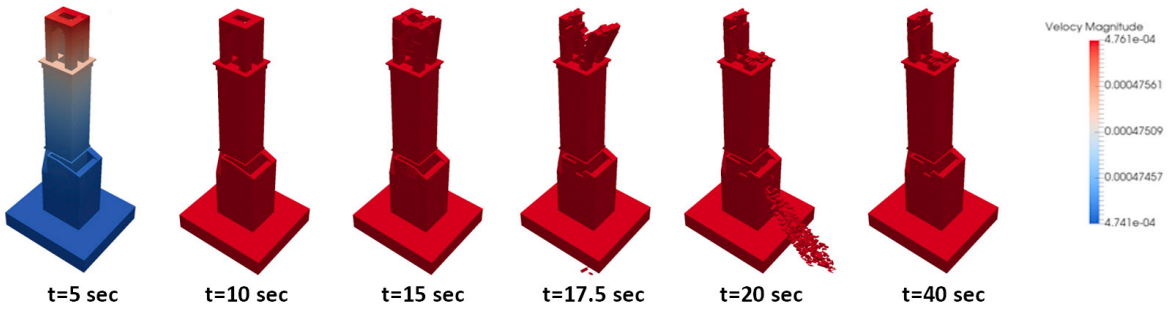

Figure 7. Numerical results with NSCD method for different time steps.

Further damage can also be read (Fig. 7) in the enlargement area at the base of the tower, where there are significant cracks along the peripheral walls, showing a restricted collapse at the top of the wall. The numerical results agree with the real damage shown by the tower following the shock of 24th August and 30th October 2016, after that the bell tower was, respectively, seriously damaged and collapsed in correspondence of the bell cell. Besides, a minimal sliding between the blocks along the longitudinal development of the tower should be highlighted. These sliding can be associated with small cracks that are scarcely visible and very localized.

As can be observed from the Fig. 7, NSCD method differs from a continuum approach, and it stands as complementary to this latter. While NSCD method takes into account an accurate description of the motions induced by the inertial masses, a continuum approach describes stress and strain distributions (Clementi et al., 2018, 2016a; F. Clementi et al., 2017b; Francesco Clementi et al., 2017; Milani and Valente, 2015a, 2015b) (F. Clementi et al., 2017a; Quagliarini et al., 2017). For this reason, in Fig. 8 are reported the expected damages, for the same time steps reported in Fig. 7, obtained with FE CDP model implemented in Abaqus©. Similar results are noticeable: heavy damage associated with the bell cell and to the enlargement wall at the base. Otherwise, there is a substantial damage along the tower that is only just visible in NSCD model and which, now, does not seem to be associated with the real damage following the seismic shocks ended on 18th January 2018.

Further analyses on the influence of the mechanical parameters of interest will be necessary in order to have a clear picture of the real observed damage.

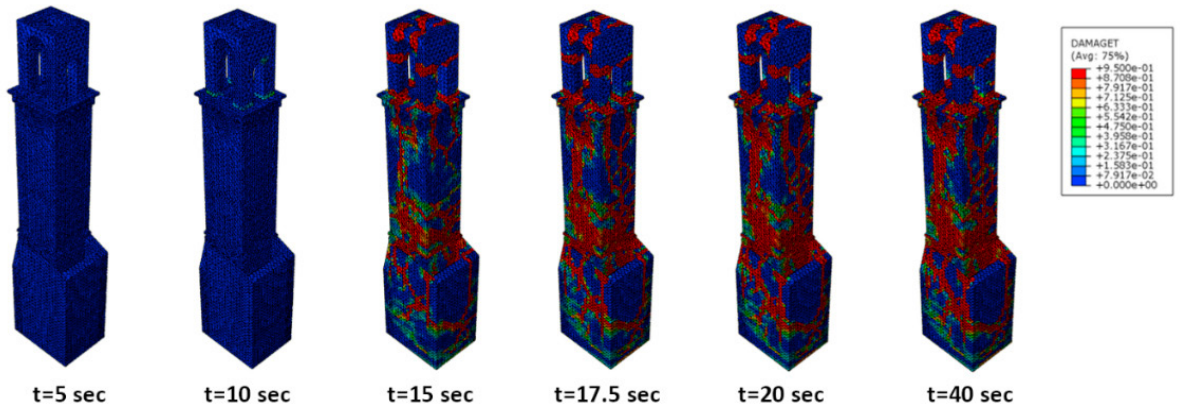

Figure 8. Numerical results with FE CDP model for different time steps.

4. Conclusions

The results obtained for the model of the civic clock tower of Amatrice (Rieti, Italy), subjected to a real earthquake excitation of 30th October 2016 that strokes Central Italy, underline the high vulnerability of this structure, especially at the upper level. The real observed damage was confirmed by two completely different mathematical models: NSCD

method (discontinuous approach) implemented in LMGC90© and CDP model (continuous approach) implemented in Abaqus©. Further comparisons are necessary especially along the development of the tower where the most considerable differences are noticed. Finally, the comparison of both methods could bring to a complete comprehension of the mechanical response of such complex structures to seismic loading, pointing out the same portions most damaged during the earthquake of 30th October 2016 (the belfry and the enlargement at the base).

Acknowledgements

The authors wish to thank Eng. Valeria Carletti for useful aid in the preliminary developments of this research.

References

Acito, M., Bocciarelli, M., Chesi, C., Milani, G., 2014. Collapse of the clock tower in Finale Emilia after the May 2012 Emilia Romagna earthquake sequence: Numerical insight. Eng. Struct. 72, 70–91. https://doi.org/10.1016/j.engstruct.2014.04.026

Circolare Ministeriale n. 617, 2009. Cons. Sup. LL. PP., "Istruzioni per l'applicazione delle Nuove Norme Tecniche per le Costruzioni" di cui al decreto ministeriale del 14.01.2008. G.U. del 26.02.2009 n. 47, supplemento ordinario n. 27. (in Italian).

Clementi, F., Gazzani, V., Poiani, M., Lenci, S., 2016a. Assessment of seismic behaviour of heritage masonry buildings using numerical modelling. J. Build. Eng. 29–47. https://doi.org/10.1016/j.jobe.2016.09.005

Clementi, F., Gazzani, V., Poiani, M., Mezzapelle, P.A., Lenci, S., 2017. Seismic Assessment of a Monumental Building through Nonlinear Analyses of a 3D Solid Model. J. Earthq. Eng. 1–27. https://doi.org/10.1080/13632469.2017.1297268

Clementi, F., Mezzapelle, P.A., Cocchi, G., Lenci, S., 2017a. Global analyses of historical masonry buildings: Equivalent frame vs. 3D solid models, in: AIP Conference Proceedings. https://doi.org/10.1063/1.4992615

Clementi, F., Nespeca, A., Lenci, S., 2016b. Seismic behavior of an Italian Renaissance Sanctuary: Damage assessment by numerical modelling, in: International Conference of Computational Methods in Sciences and Engineering 2016, ICCMSE 2016. Athens, p. 130004. https://doi.org/10.1063/1.4968722

Clementi, F., Pierdicca, A., Formisano, A., Catinari, F., Lenci, S., 2017b. Numerical model upgrading of a historical masonry building damaged during the 2016 Italian earthquakes: the case study of the Podestà palace in Montelupone (Italy). J. Civ. Struct. Heal. Monit. 7, 703–717. https://doi.org/10.1007/s13349-017-0253-4

Clementi, F., Pierdicca, A., Milani, G., Gazzani, V., Poiani, M., Lenci, S., 2018. Numerical model upgrading of ancient bell towers monitored with a wired sensors network, in: Milani, G., Taliercio, A., Garrity, S. (Ed.), 10th International Masonry Conference (IMC_10). Milano, pp. 1–11.

Clementi, F., Quagliarini, E., Monni, F., Giordano, E., Lenci, S., 2017c. Cultural Heritage and Earthquake: The Case Study of "Santa Maria della Carità" in Ascoli Piceno. Open Civ. Eng. J. 11, 1079–1105. https://doi.org/10.2174/1874149501711011079

Dhanasekar, M., Page, A., Kleeman, P., 1985. The failure of brick masonry under biaxial stresses. Proc. Inst. Civ. Eng. 79, 295–313. https://doi.org/10.1680/iicep.1985.992

Fiorentino, G., Forte, A., Pagano, E., Sabetta, F., Baggio, C., Lavorato, D., Nuti, C., Santini, S., 2018. Damage patterns in the town of Amatrice after August 24th 2016 Central Italy earthquakes. Bull. Earthq. Eng. 16, 1399–1423. https://doi.org/10.1007/s10518-017-0254-z

Italian Department of Civil Protection, 2017. 2016 Central Italy earthquake. URL http://www.protezionecivile.gov.it/jcms/it/terremoto_centro_italia_2016.wp

Jean, M., 1999. The non-smooth contact dynamics method. Comput. Methods Appl. Mech. Eng. 177, 235–257. https://doi.org/10.1016/S0045-7825(98)00383-1

Lee, J., Fenves, G.L., 1998. Plastic-Damage Model for Cyclic Loading of Concrete Structures. J. Eng. Mech. 124, 892–900. https://doi.org/10.1061/(ASCE)0733-9399(1998)124:8(892)

Milani, G., Lourenço, P.B., Tralli, A., 2006. Homogenised limit analysis of masonry walls, Part I: Failure surfaces. Comput. Struct. 84, 166–180. https://doi.org/10.1016/j.compstruc.2005.09.005

Milani, G., Valente, M., 2015a. Failure analysis of seven masonry churches severely damaged during the 2012 Emilia-Romagna (Italy) earthquake: Non-linear dynamic analyses vs conventional static approaches. Eng. Fail. Anal. 54, 13–56. https://doi.org/10.1016/j.engfailanal.2015.03.016

Milani, G., Valente, M., 2015b. Comparative pushover and limit analyses on seven masonry churches damaged by the 2012 Emilia-Romagna (Italy) seismic events: Possibilities of non-linear finite elements compared with pre-assigned failure mechanisms. Eng. Fail. Anal. 47, 129–161. https://doi.org/10.1016/j.engfailanal.2014.09.016

Moreau, J.J., 1988. Unilateral Contact and Dry Friction in Finite Freedom Dynamics, in: Nonsmooth Mechanics and Applications. Springer Vienna, Vienna, pp. 1–82. https://doi.org/10.1007/978-3-7091-2624-0_1

Pluijm, R. Van Der, Rutten, H., Ceelen, M., 2000. Shear Behaviour of Bed Joints. 12th Int. Brick/Block Mason. Conf. 1849–1862.

Quagliarini, E., Maracchini, G., Clementi, F., 2017. Uses and limits of the Equivalent Frame Model on existing unreinforced masonry buildings for assessing their seismic risk: A review. J. Build. Eng. 10, 166–182. https://doi.org/10.1016/j.jobe.2017.03.004

Valente, M., Milani, G., 2016. Seismic assessment of historical masonry towers by means of simplified approaches and standard FEM. Constr. Build. Mater. 108, 74–104. https://doi.org/10.1016/j.conbuildmat.2016.01.025

Vasconcelos, G., Lourenço, P.B., 2009. Experimental characterization of stone masonry in shear and compression. Constr. Build. Mater. 23, 3337–3345. https://doi.org/10.1016/j.conbuildmat.2009.06.045